Alternative Shaker transcripts express either rapidly inactivating or noninactivating K$^+$ channels

(potassium channel/delayed rectifier/*Drosophila*/cRNA expression/*Xenopus* oocyte)

M. Stocker*, W. Stühmer†, R. Wittka‡, X. Wang†, R. Müller*, A. Ferrus§, and O. Pongs*

*Lehrstuhl für Biochemie and ‡AG biophys. Chemie von Membranen, Ruhr-Universität Bochum, D-4630 Bochum, Federal Republic of Germany; †Max-Planck-Institut für biophysikalische Chemie, D-3400 Göttingen, Federal Republic of Germany; and §Instituto Cajal, E-28002 Madrid, Spain

ABSTRACT   Two members of the Shaker K$^+$ channel family designated ShA2 and ShD2 were characterized in the *Xenopus* oocyte expression system. The predicted amino acid sequences of ShA2 and ShD2 differ only in the amino terminus, which is located intracellularly according to the present topological model of K$^+$ channels. The differing amino termini have profound effects on the electrophysiological and pharmacological properties of the K$^+$ channel. Most markedly, the nature of the amino terminus determines whether the K$^+$ channel mediates rapidly inactivating or noninactivating K$^+$ currents. It also affects the 4-aminopyridine, tetraethylammonium, and charybdotoxin sensitivities of the K$^+$ channels. These results suggest that the amino terminus of Shaker proteins affects K$^+$ channel structures on both sides of the membrane.

Voltage-gated K$^+$ channels represent an extraordinarily diverse class of ionic channels that are essential for setting the membrane resting potential and the duration of action potentials and for the generation and tuning of firing patterns (1, 2). Several invertebrate and vertebrate voltage-gated K$^+$ channels have been cloned (3–14). Their primary sequences are remarkably similar despite the functional diversity of K$^+$ channels. Apparently, voltage-gated K$^+$ channels with different electrophysiological and pharmacological properties have been derived from a common ancestor (11, 12). Comparison of the sequences and the electrophysiological properties of cloned K$^+$ channels suggests that minor sequence alterations sufficed to build a variety of diverse voltage-gated K$^+$ channels.

The cloning and functional characterization of the *Drosophila* Shaker (Sh) K$^+$ channel family revealed variant transient A-type K$^+$ channels with distinct activation and inactivation rates (15–17). The K$^+$ channels are formed by proteins that share a common core region containing six potentially membrane-spanning segments flanked by diverse amino and carboxyl termini. It has been proposed that the six transmembrane segments are oriented in a pseudosymmetric fashion across the membrane and that the amino and carboxyl termini are located on the intracellular side of the membrane (4). Given the proposed topology of K$^+$ channels in the membrane, the amino-terminal sequence of Sh protein might be operative only at the intracellular side of the membrane. In the present report, we show that a particular variation of the amino-terminal sequence in the Sh protein family affects the electrophysiological as well as the pharmacological properties of Sh K$^+$ channels. This variation transforms rapidly inactivating Sh K$^+$ channels into noninactivating ones. Also, the sensitivity toward channel blockers and toxins acting from the outside is altered by 1–2 orders of magnitude. These results suggest that the amino-terminal sequences of Sh proteins affect structures of the Sh K$^+$

channels with functional roles on both sides of the membrane.

MATERIALS AND METHODS

RNA Synthesis and Injection into Oocytes. A full-length cDNA clone (ShcDNAβ) encoding ShA2 has been described (4). Since a full-length cDNA clone encoding ShD2 has not been isolated to date, overlapping cDNA clones encoding partial sequences were used to construct templates for cRNA synthesis. The pAS18 expression vector (18) was used for expression. We constructed pAS18-β$_E$, a clone that contained the core region (exons 7–15 in ref. 4) and the carboxyl terminus (exons 16–18 in ref. 4) shared by all members of the class 2 Sh family (see Fig. 1). This clone was obtained by ligating the *Xba* I–*Eco*RI fragment of cDNAβ (nucleotides +699 to +2151 in ref. 4) with *Xba* I/*Sma* I-cut pAS18 after the *Eco*RI site of the *Xba* I–*Eco*RI fragment of cDNAβ was filled in with DNA polymerase I (Klenow). Various cDNAs encoding the different amino termini of Sh proteins were ligated with *Hind*III/*Xba* I-cut pAS18-β$_E$ DNA. For this purpose the *Hind*III site was filled in with DNA polymerase I (Klenow). pAS18-A2 was obtained by ligating the *Hind*III/*Xba* I-cut pAS18-β$_E$ DNA with the *Eco*RI–*Xba* I fragment of cDNAβ (nucleotides −270 to +699 in ref. 4) after filling in its *Eco*RI site. pAS18-D2 was obtained by ligating the *Eco*RI/*Xba* I-cut pAS18-β$_E$ DNA with the *Eco*RI–*Xba* I fragment of cDNAδ (nucleotides −73 to 600 in ref. 4) blunt-ended at its *Eco*RI site. The resulting pAS18-A2 and pAS18-D2 clones were verified by restriction enzyme digestions. pAS18-A2 and pAS18-D2 plasmid DNAs were linearized at the *Eco*RI site before synthesis of ShA2 and ShD2 cRNAs. cRNA synthesis was as described (18, 19). cRNA (0.5 mg/ml) was injected into oocytes of *Xenopus laevis* (stage Vb/VI) in portions of 50 nl per oocyte. The oocytes were incubated in Barth's medium at 19°C and prepared for electrophysiological measurements (20). The expression of Sh K$^+$ channels was detectable in nearly every oocyte 2 days after injection, with a maximum at days 4–7.

Current Recording and Data Analysis. The bath solution was 115 mM NaCl/2.5 mM KCl/1.8 mM CaCl$_2$/10 mM Hepes, pH 7.2. In some experiments, Na$^+$ was partially replaced by K$^+$ or by the blocking substances 4-aminopyridine (4-AP) and tetraethylammonium chloride (TEA) (Sigma). Dendrotoxin (DTX), mast cell degranulating peptide (MCDP) (gifts from F. Dreyer and E. Habermann, Universität Giessen, Giessen, F.R.G.), and charybdotoxin (CTX) (gift from C. Miller, Brandeis University, Waltham, MA) were added to the bath solution. Patches in the inside-out configuration were excised into 120 mM KCl/1.8 mM EGTA–KOH/10 mM Hepes, pH 7.2.

Abbreviations: 4-AP, 4-aminopyridine; TEA, tetraethylammonium; DTX, dendrotoxin; MCDP, mast cell degranulating peptide; CTX, charybdotoxin.

A two-microelectrode voltage clamp was used to test for the action of the toxins and to determine the whole-cell K^+ current of each oocyte prior to patch current recording. All values given are means ± SD. In ≈20% of the oocytes injected the current was >10 μA for a test pulse from −80 to 0 mV. This indicated that the channel density was high enough for recording from macropatches. Pipettes for macropatches were made from aluminum silicate glass with a tip diameter of 4–6 μm (21). They were filled with the normal bath solution for cell-attached recording, giving a resistance of 0.5–1 MΩ. The intracellular potential was simultaneously measured by a microelectrode to determine the effective transmembrane potential across the patch. The K^+ channel density was not homogeneous, and therefore the oocyte had to be patched on several different places before an area of high current density was found. Stimulation and sampling were done as described (21). To determine the steady-state activation parameters, the function $G = G_{max}/\{1 + \exp[(V_{1/2} - V)/a]\}$ was fitted to the conductance values (G) at each potential. These conductances were obtained by dividing the peak current by the driving force, assuming a reversal potential of −100 mV in the cell-attached configuration and a calculated reversal of −98 mV in the inside-out configuration. Steady-state inactivation parameters were measured for the only channel inactivating in the millisecond time scale, ShA2, by using prepulses lasting 1 s. The data were analyzed by fitting the function $I/I_{max} = 1/\{1 + \exp[(V - V_{1/2})/a]\}$ to the data points.

Pipettes for single-channel recording were made from borosilicate glass and had resistances of 3–5 MΩ when filled with bath solution. The single-channel current records were stored on video tape and analyzed by an interactive semi-automatic procedure. Distributions of single-channel current amplitudes were fitted assuming Gaussian distribution.

RESULTS

The *Sh* locus encodes a large transcription unit that is spliced into multiple mature transcripts (3, 4, 7). These transcripts are translated into a family of K^+ channel-forming proteins that have five variant amino termini and two different carboxyl termini (Fig. 1). The nomenclature of Sh K^+ channels poses potential problems. Historically, it is based on isolated cDNA clones, which have been characterized in three different laboratories (3, 4, 7). We have proposed a systematic nomenclature that designates predicted Sh K^+ channel-forming proteins and not cDNA clones (22). The nomenclature (Fig. 1) considers only those Sh proteins which have

been shown to mediate K^+ currents. The variant amino termini are designated A, B, D, G, and H according to the corresponding cDNAs (see legend to Fig. 1). The two alternative carboxyl termini are designated by 1 or 2; e.g., ShA1 protein contains amino terminus A and carboxyl terminus 1. The ability of ShD proteins to form K^+ channels had not been studied yet. We became interested in ShD proteins because polymerase chain reaction and Northern analysis of ShD transcripts indicated that ShD transcripts are preferentially expressed in *Drosophila* body tissue (data not shown), whereas other members of the Sh family are preferentially expressed in the nervous system (4). Also, the deduced ShD2 protein sequence had the highest homology with the deduced sequence of rat RCK1 protein (12), which forms delayed rectifier-type K^+ channels in the *Xenopus* oocyte expression system (10, 13, 19).

ShA2- and ShD2-Mediated Currents Differ in Activation and Inactivation Kinetics. ShA2 channels mediate the most rapidly inactivating outward currents of the Sh K^+ channel family (refs. 16 and 17; Fig. 2). The 61 amino-terminal amino acids of ShA2 are replaced by only 16 amino acids in ShD2 (4, 22). This replacement changes the activation and inactivation kinetics of macroscopic currents produced by ShA2 or ShD2 after injection of the respective cRNAs into *Xenopus* oocytes. The rise-to-peak of the ShA2 current for a test pulse from a holding potential of −80 mV to a test potential of 10 mV required 1.4 ± 0.5 ms ($n = 9$). ShA2 currents inactivated rapidly with a time course that could be fitted with a single exponential, but the currents did not fall to baseline at the end of a 100-ms test pulse (Fig. 2a). A residual steady-state current representing 8–15% ($n = 10$) of the transient peak current was observed. It did not inactivate within the millisecond time range.

The normalized conductance–voltage relation (Fig. 2b) of the ShA2 ensemble currents, $G/G_{max}(V)$, indicates that they start to activate at test potentials of −40 mV. The conductance was half-maximal in the range of test potentials of −14.5 ± 9.8 mV (Table 1) and saturated at test potentials of +30 to +40 mV. The slope of the normalized conductance–voltage relation is 13.2 mV/e-fold. The results were obtained from macropatches by recording in the cell-attached configuration of the patch-clamp technique. They are similar to results obtained with whole-cell current recordings after injection of similar Sh transcripts (ShB/ShH4) into oocytes (15–17). In inside-out patches the values for half-maximal activation and its slope were −23.6 and 16.7 mV/e-fold, respectively. Steady-state inactivation of the ShA2 currents measured in the cell-attached mode was also similar to that
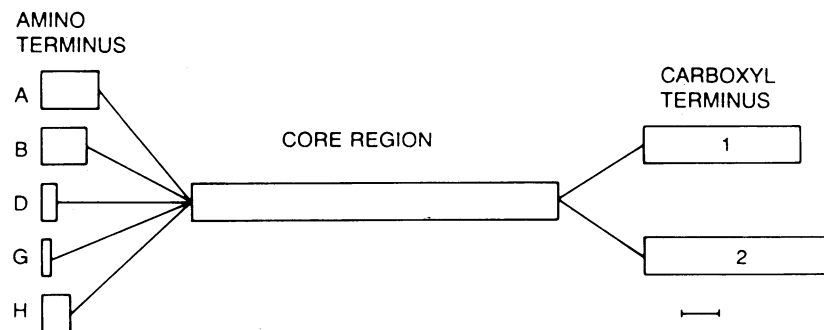

FIG. 1. General structure of the family of Sh K^+ channels. Boxes illustrate the various domains of Sh K^+ channel-forming proteins. A common core region is flanked by variable amino termini (A, B, D, G, H) and by one of two alternative carboxyl termini (22). Box lengths are approximately to scale. Bar at lower right corresponds to 20 amino acids. All combinations between the core region and the amino and carboxyl termini are possible (7, 22). The amino-terminal sequence derived from Sh cDNAα has been designated A, that of cDNAβ (4) B, of cDNAγ (4) G, of cDNAδ (4) D, and of cDNA H37 (7) H, respectively. The suffix 1 or 2 designates the carboxyl terminus; e.g., ShA2 is a protein with amino terminus A and carboxyl terminus 2. The expression of transient voltage-gated A-type currents was studied with ShA1, ShA2, ShB2, ShC1, and ShH1 transcripts after injection into *Xenopus* oocytes. [Code for the nomenclature of other laboratories: ShA1 = ShA (3, 16); ShA2 = ShB (3, 16) or ShH4 (7, 17); ShB2 = ShD (3, 16); ShC1 = ShC (3, 16); ShH1 = ShH37 (7, 17)].
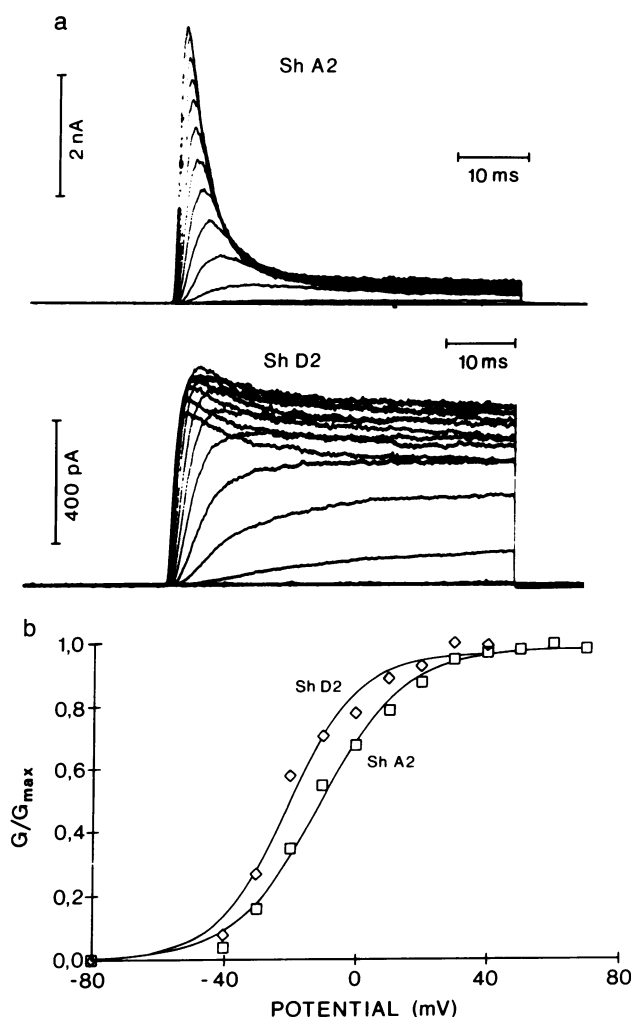
FIG. 2. (*a*) Families of outward currents in response to depolarizing voltage steps recorded from a macropatch in the cell-attached configuration. Top ShA2; bottom ShD2. The traces are responses to 50-ms voltage steps from −80 to 80 mV in 10-mV increments from a holding potential of −100 mV. Sampling interval was 60 μs; filtering was at 3 kHz (3 dB), low pass. (*b*) Plots of normalized conductance (G/G_{max}) versus test potential for ShA2 (□) and ShD2 (◇) channels. The conductance values were obtained by dividing the peak current at a particular test potential by an assumed reversal potential of −100 mV (close to the potential where tail currents reverse). The continuous lines are the results of nonlinear least-squares fits to the data. The maximal conductance (G_{max}) obtained by the fit was used to normalize the data.

Table 1. Electrophysiological parameters of ShA2 and ShD2 channels expressed in *Xenopus* oocytes

cRNA	Method	Activation			Inactivation		
		$V_{1/2}$, mV	a, mV	n	$V_{1/2}$, mV	a, mV	n
ShA2	CA	−14.5 ± 9.81	13.2	9	−34.1 ± 2.7	6.4	2
	IO	−23.6	16.7	1	−50.3 ± 2.7	6.5	3
ShD2	CA	−25.6 ± 6.97	11.4	5			
	IO	−36.4	8.33	1			

CA, cell-attached patches; IO, inside-out patches; $V_{1/2}$, potential of half-activation or inactivation; a, potential change needed to obtain an e-fold change in the conductance- or inactivation-voltage dependencies at $V_{1/2}$.

conductance saturated at 0 to +10 mV. The slope of the normalized conductance–voltage relations is 11.4 mV/e-fold. The ShD2 currents needed 2.5 ± 0.6 ms ($n = 5$) to rise to peak following a test pulse from a holding potential of −80 mV to a potential of 10 mV. This difference in activation rates could mean that ShD2 currents activate more slowly than ShA2 currents. However, as shown in the *Discussion*, variations in inactivation rates *per se* are able to reproduce these changes in rise times.

ShA2 and ShD2 Channels Have Similar Conductances and Different Open Durations. Examples of single-channel currents recorded in inside-out patches from oocytes injected with ShA2 or ShD2 cRNA are shown in Fig. 3. With a driving force of 100 mV, both unitary currents showed a Gaussian distribution around a mean of ≈0.8 pA, giving an apparent single-channel conductance of ≈8 pS. This agrees with data for other Sh K⁺ channels (17, 24), indicating that the amino terminus does not greatly affect the single-channel conductance of Sh K⁺ channels. Further, the selectivity of the K⁺ channels, as determined from tail-current analysis, was not altered (data not shown). Open-duration histograms of both channels at 0 mV are well fitted by single-exponential probability density functions, with means of 0.7 ms in the case of ShA2 channels and of 3.0 ms in the case of ShD2 channels.

ShA2 and ShD2 Channels Have Different Pharmacological Properties. The proposed membrane topology of voltage-gated ion channels places the amino terminus on the intracellular side of the membrane. Therefore, the differences in the gating behavior of ShA2 and ShD2 channels might indicate a different interaction of the A or D amino terminus with the inactivation gate of the Sh K⁺ channel located intracellularly (25). The structural differences between ShA2 and ShD2 channels could be purely local. Alternatively, the different amino termini could influence the overall structure of Sh K⁺ channels. This proposition was tested with K⁺ channel blockers. Because of its positive charge and polar nature, CTX is membrane-impermeant and acts from the extracellular side. The affinity of CTX for its extracellular K⁺ channel binding site should not be influenced if the structural differences between ShA2 and ShD2 channels were confined to the intracellular side of the channel. However, the amplitudes of currents measured in oocytes injected with ShA2 or ShD2 cRNA were reduced by different concentrations of CTX (Table 2). ShA2 channels were very sensitive to CTX (IC$_{50}$ = 4 nM) in agreement with previously published data (26). In contrast, ShD2 channels were relatively insensitive to CTX (IC$_{50}$ = 105 nM), more like native Sh K⁺ channels (24). The different CTX sensitivities of ShA2 and ShD2 channels indicate that the two channels differ in extracellular structure. This observation is further supported by the different sensitivities of ShA2 and ShD2 channels to other K⁺ channel blockers that probably also act from the extracellular side (Table 2). ShA2 channels were 5 times more sensitive to TEA (IC$_{50}$ = 18 mM) than ShD2 channels (IC$_{50}$ = 92 mM). On the other hand, ShA2 channels were only 1/10th as sensitive to 4-AP (IC$_{50}$ = 5 mM) as the ShD2 channels (IC$_{50}$ = 0.5 mM).

of ShB/ShH4 currents, both in voltage dependence and in slope (Table 1). On excision of the patch, all electrophysiological parameters measured shifted to the left on the voltage axis. These shifts cannot be explained by changes in junction potential, which were on the order of only a few millivolts.

In contrast to ShA2 currents, ShD2 currents did not inactivate rapidly at most test potentials studied (Fig. 2*a*). Only at more positive test potentials, where the noninactivating ShD2 steady-state current saturates, did a rapidly inactivating component become apparent. At test potentials of +80 mV, the rapidly inactivating component represented 15 ± 10% ($n = 5$) of the peak current. The appearance of this rapidly inactivating component was accompanied by a decrease in steady-state current. The $G/G_{max}(V)$ relation of ShD2 indicates that channels began to activate at test potentials of −40 mV (Fig. 2*b*), like ShA2 currents. However, the conductance was half-maximal at −25.6 ± 7 mV (Table 1), ≈10 mV more negative than that of ShA2 currents. The
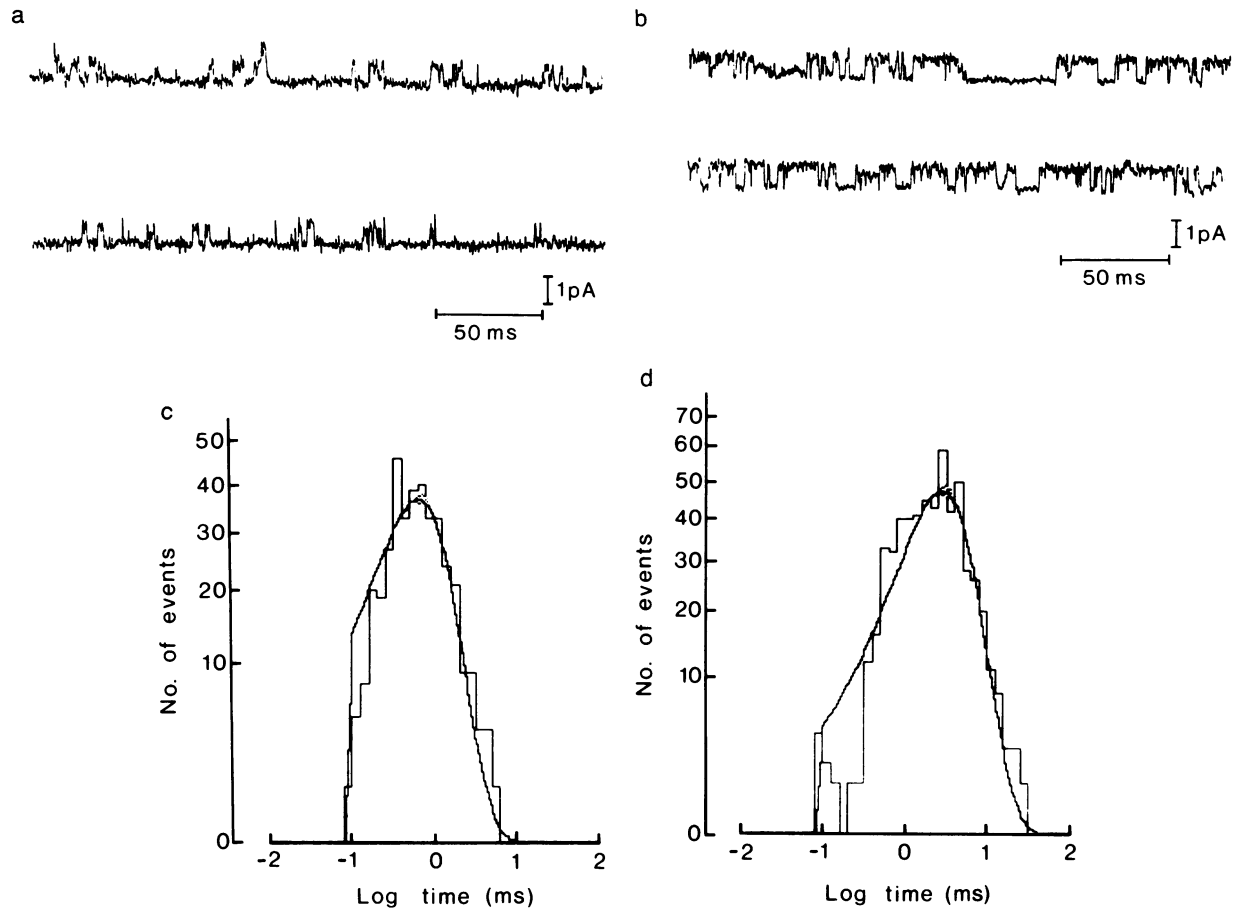
FIG. 3.   (*a* and *b*) Single ShA2 (*a*) and ShD2 (*b*) channels recorded in an inside-out patch from oocytes injected with ShA2 or ShD2 cRNA, respectively. The data have been transformed for improved display according to ref. 23. Representative sweeps containing channel openings during a prolonged depolarization to 0 mV are shown. The lower part of each trace represents the closed current level. (*c* and *d*) Open-duration histogram at 0 mV for ShA2 channels, (*c*), giving a mean open time of 0.7 ms, and for ShD2 channels (*d*), giving a mean open time of 3.0 ms.

These different pharmacological properties of ShA2 and ShD2 channels indicate that the replacement of the A terminus by the D terminus in Sh K^+ channels produces a conformational change that affects several binding sites for K^+ channel blockers as well as the gating behavior of the K^+ channels. Finally, it should be noted that both ShA2 and ShD2 channels were insensitive to DTX and the MCDP (Table 2), in strong contrast to most members of the RCK K^+ channel family (10).

DISCUSSION

Electrophysiological data on voltage-dependent K^+ channels indicate that the activation/inactivation gate(s) of these channels is located on the intracellular side of the membrane and the toxin binding sites on the extracellular side (2, 26). Tables 1 and 2 show that ShA2 channels differ from ShD2 channels both electrophysiologically and pharmacologically. When all

Table 2.   Pharmacological characteristics of ShA2 and ShD2 channels expressed in *Xenopus* oocytes

cRNA	4-AP, mM	TEA, mM	DTX, nM	MCDP, nM	CTX, nM
			IC$_{50}$ value		
ShA2	5.5	17.8	>>200	>>2000	4.0
ShD2	0.5	92	>>200	>>1000	105.0

IC$_{50}$ values (concentrations for 50% inhibition of peak current) were measured at a test potential of +20 mV; all experiments were made under two-electrode voltage clamp. Each value is the average of at least two independent measurements.

the observed differences are considered, the K^+ channel structures involved in channel gating as well as the different binding sites for channel blockers ought to be different between ShA2 and ShD2 channels. It should be realized that the electrophysiological and pharmacological changes introduced by the variant amino termini are neither necessarily nor specifically linked to these sequences. It is known that a local structural change can trigger a change in the quaternary protein structure (27). The available evidence suggests that Sh K^+ channels are multimeric proteins and consequently have a quaternary structure (4, 28). We propose, therefore, that the local change in the amino-terminal sequence of a Sh channel alters the quaternary structure of the K^+ channel and thereby affects its electrophysiological and pharmacological properties. In this context one has to consider the possibility that changes in inactivation properties might change K^+-site occupancy and thereby change toxin equilibrium constants on the extracellular side [a similar effect has been observed in Ca^{2+}-activated K^+ channels for CTX binding (29)]. The altered quaternary structure does not, however, affect the single-channel conductance and ion selectivity, which are properties of the pore.

The different gating properties of ShA2 and ShD2 channels can be described in general terms by a simple kinetic model,

$$C \underset{\delta}{\overset{\gamma}{\rightleftharpoons}} O \underset{\lambda}{\overset{\kappa}{\rightleftharpoons}} I,$$
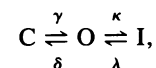
in which C is the last, short-duration closed state, O a short-duration open state, and I a long-duration inactivated state (λ is assumed to be very small). The distribution of open

times will be a single exponential with a mean duration of $1/(\delta + \kappa)$, and the level of steady-state inactivation will depend on the ratio between κ and λ. Since the experimental data indicate that both $\delta + \kappa$ and the ratio between κ and λ vary between ShA2 and ShD2, the most economical interpretation of our results can be obtained by assuming that the amino termini influence mainly the rate κ. The rapidly inactivating currents of ShA2 channels and their short mean open times indicate that κ is large. On the other hand, ShD2 channels mediate noninactivating currents with longer mean open times, indicating that κ is small. In fact, the current records obtained at 0 mV could be simulated by assuming the following rates (ms^{-1}): $\gamma = 0.40$, $\delta = 0.32$, and $\lambda = 0.05$ for both Sh channels, and either $\kappa = 1.11$ for ShA2 or $\kappa = 0.013$ for ShD2. These parameters give the experimentally determined mean open durations of 0.7 ms for ShA2 and 3.0 ms for ShD2 and are also able to reproduce quantitatively the activation and inactivation time constants as well as the steady-state inactivation levels.

Intermediate values of κ emulated currents with various degrees of rapidly inactivating as well as noninactivating components, similar to the ones observed in expression studies with ShB and ShG channels (16, 17) or in variants generated by *in vitro* mutagenesis (30). In experiments with tissue-derived mRNA or with intact cells, the presence of various inactivating components would be explained by the probable presence of more than one channel type. In the present case, however, only one channel species is present, and the kinetic model given above is able to emulate the various inactivation kinetics. In this context it is interesting to compare the inactivation behavior of Sh K$^+$ channel variants with that of the Na$^+$ channel. This channel consists of four domains, each of which is homologous to the K$^+$ channel subunit (4). Manipulations of the region between repeats III and IV drastically influence the inactivation properties of the Na$^+$ channel (31). Antibodies directed against this region also selectively affect inactivation (32). The sequence between domains III and IV is formally equivalent to the carboxyl- and amino-terminal sequences of one K$^+$ channel subunit. This can be taken as an indication that these regions are able to modulate inactivation in both types of channels.

Sh K$^+$ channels expressed in the oocyte expression system are similar to native Sh K$^+$ channels (24) in many respects—e.g., voltage dependence of activation/inactivation and single-channel conductance—but they differ in some properties—e.g., open duration times of single channels and sensitivity to CTX. Native Sh K$^+$ channels are insensitive to CTX, whereas Sh K$^+$ channels expressed in *Xenopus* oocytes are very sensitive to CTX (ref. 33 and Table 2). The present study shows that the CTX sensitivity of homomultimeric Sh K$^+$ channels is variable. At 50 nM CTX, currents mediated by ShA2 or ShD2 channels are either blocked completely or not blocked at all, respectively. This CTX concentration was used previously to study the CTX sensitivity of native Sh K$^+$ channels (24). The different pharmacological properties of ShA2 and ShD2 proteins can be reconciled by assuming more than one open state with different affinities for the various channel blockers. As a consequence, variant dwell times in the various states would give rise to diverse inhibition doses. However, that the open-time distribution is well fitted by a single exponential is inconsistent with this hypothesis. Alternatively, the variant pharmacological properties of ShA2 and ShD2 could arise from parts of the amino terminus located extracellularly. The absence of a signal peptide mediating membrane translocation of the amino terminus in all voltage-

dependent channels sequenced so far, as well as topological constraints on the homologous Na$^+$ channel (31, 32), argues against this hypothesis.

1. Hille, B. (1984) *Ionic Channels of Excitable Membranes* (Sinauer, Sunderland, MA).
2. Rudy, B. (1988) *Neuroscience* **25**, 729–750.
3. Schwarz, T. L., Tempel, B. L., Papazian, D. M., Jan, Y. N. & Jan, L. Y. (1988) *Nature (London)* **331**, 137–142.
4. Pongs, O., Kecskemethy, N., Müller, R., Krah-Jentgens, I., Baumann, A., Kiltz, H. H., Canal, I., Llamazares, S. & Ferrus, A. (1988) *EMBO J.* **7**, 1087–1096.
5. Tempel, B. L., Jan, Y. N. & Jan, L. Y. (1988) *Nature (London)* **332**, 837–839.
6. Butler, A., Wei, A., Baker, K. & Salkoff, L. (1989) *Science* **243**, 943–947.
7. Kamb, A., Tseng-Crank, J. & Tanouye, M. A. (1988) *Neuron* **1**, 421–430.
8. Frech, G. C., Van Dongen, A. M., Schuster, G., Brown, A. M. & Joho, R. H. (1989) *Nature (London)* **340**, 642–645.
9. McKinnon, D. (1989) *J. Biol. Chem.* **264**, 8230–8236.
10. Stühmer, W., Ruppersberg, J. P., Schröter, K. H., Sakmann, B., Stocker, M., Giese, K. P., Perschke, A., Baumann, A. & Pongs, O. (1989) *EMBO J.* **8**, 3235–3244.
11. Yokoyama, S., Imoto, K., Kawamura, T., Higashida, H., Iwabe, N., Miyata, T. & Numa, S. (1989) *FEBS Lett.* **259**, 37–42.
12. Baumann, A., Grupe, A., Ackermann, A. & Pongs, O. (1988) *EMBO J.* **7**, 2457–2463.
13. Christie, M. J., Adelman, J. P., Douglass, J. & North, R. A. (1989) *Science* **244**, 221–224.
14. Chandy, K. G., Williams, C. B., Spencer, R. H., Aguilar, B. A., Ghanshani, S., Tempel, B. L. & Gutman, G. A. (1990) *Science* **247**, 973–975.
15. Timpe, L. C., Schwarz, T. L., Tempel, B. L., Papazian, D. M., Jan, Y. N. & Jan, L. Y. (1988) *Nature (London)* **331**, 143–145.
16. Timpe, L. C., Jan, Y. N. & Jan, L. Y. (1988) *Neuron* **1**, 659–667.
17. Iverson, L. E., Tanouye, M. Y., Lester, H. A., Davidson, N. & Rudy, B. (1988) *Proc. Natl. Acad. Sci. USA* **85**, 5723–5727.
18. Krieg, P. A. & Melton, D. A. (1984) *Nucleic Acids Res.* **12**, 7057–7070.
19. Stühmer, W., Stocker, M., Sakmann, B., Seeburg, P., Baumann, A., Grupe, A. & Pongs, O. (1988) *FEBS Lett.* **242**, 199–206.
20. Methfessel, C., Witzemann, V., Takahashi, T., Mishina, M., Numa, S. & Sakmann, B. (1986) *Pflügers Arch. Gesamte Physiol.* **407**, 577–588.
21. Stühmer, W., Methfessel, C., Sakmann, B., Noda, M. & Numa, S. (1987) *Eur. Biophys. J.* **14**, 131–138.
22. Baumann, A., Krah-Jentgens, I., Müller, R., Müller-Holtkamp, F., Canal, I., Galceran, F., Ferrus, A. & Pongs, O. (1989) in *Molecular Biology of Neuroreceptors and Ion Channels*, ed. Maelicke, A., (Springer, Berlin), pp. 231–244.
23. Sigworth, F. J. & Sine, M. (1987) *Biophys. J.* **52**, 1047–1054.
24. Zagotta, W. N., Germeraad, S., Garber, S. S., Hoshi, T. & Aldrich, R. (1989) *Neuron* **3**, 773–782.
25. Armstrong, C. M. (1969) *J. Gen. Physiol.* **54**, 553–575.
26. McKinnon, R. & Miller, C. (1989) *Science* **245**, 1382–1385.
27. Perutz, M. F., Fermi, G., Luisi, B., Shaaman, B. & Liddington, R. C. (1987) *Acc. Chem. Res.* **20**, 309–321.
28. Gisselmann, G., Sewing, S., Madsen, B. W., Mallart, A., Angaut-Petit, D., Müller-Holtkamp, F., Ferrus, A. & Pongs, O. (1989) *EMBO J.* **8**, 2359–2364.
29. McKinnon, R. & Miller, C. (1988) *J. Gen. Physiol.* **91**, 335–349.
30. Hoshi, T., Zagotta, W. N. & Aldrich, R. W. (1989) *Neurosci. Abstr.* **15**, 338.
31. Stühmer, W., Conti, F., Suzuki, H., Wang, X., Noda, M., Yahagi, N., Kubo, H. & Numa, S. (1989) *Nature (London)* **339**, 597–603.
32. Vassilev, P., Scheuer, T. & Catterall, W. A. (1989) *Proc. Natl. Acad. Sci. USA* **86**, 8147–8151.
33. McKinnon, R., Reinhart, P. & White, M. M. (1988) *Neuron* **3**, 773–782.